研究成果の刊行に関する一覧表

書　籍

著者氏名	論文タイトル名	書籍全体の編集者名	書籍名	出版社名	出版地	出版年	ページ
堀江　稔	遺伝性不整脈 4．QT延長症候群	相澤　義房	新しい診断と治療のABC 循環器11 心臓突然死	最新医学社	大阪	2009	105-112
堀江　稔	QT延長症候群	小室　一成	循環器疾患のサイエンス	南山堂	東京	2010	155-159

雑　誌

発表者氏名	論文タイトル名	発表誌名	巻号	ページ	出版年
Yasuda S, Hiramatsu S, Odashiro K, Maruyama T, Tsuji K, Horie M.	A family of hereditary long QT syndrome caused by Q738X HERG mutation.	Int J Cardiol.		in press	
Yamamura K, Muneuchi J, Uike K, Ikeda K, Inoue H, Takahata Y, Shiokawa Y, Yoshikane Y, Makiyama T, Horie M, Hara T.	A novel SCN5A mutation associated with the linker between III and IV domains of Na(v)1.5 in a neonate with fatal long QT syndrome.	Int J Cardiol.		in press	
Watanabe H, Makiyama T, Koyama T, Kannankeril PJ, Seto S, Okamura K, Oda H, Itoh H, Okada M, Tanabe N, Yagihara N, Kamakura S, Horie M, Aizawa Y, Shimizu W.	High prevalence of early repolarization in short QT syndrome.	Heart Rhythm	7	647-652	2010
Ishida K, Hayashi H, Miyamoto A, Sugimoto Y, Ito M, Murakami Y, Horie M	P-wave and the development of atrial fibrillation.	Heart Rhythm	7	289-294	2010
Ozeki Y, Fujii K, Kuromoto N, Yamada N, Okawa M, Aoki T, Takahashi J, Narita M, Ishida N, Saito O, Horie M, Kunugi H	QTc prolongation and antipsychotic medication in 1017 patients with schizophrenia.	Prog Neuropsychopharmacol Biol Psychiatry	34	401-405	2010
Horigome H, Nagashima M, Sumitomo N, Yoshinaga M, Ushinohama H, Iwamoto M, Shiono J, Ichihashi K, Hasegawa S, Yoshikawa T, Matsunaga T, Goto H, Waki K, Arima M, Takasugi H, Tanaka Y, Miura M, Ogawa K, Suzuki H, Yamagishi H, Ikoma M, Suda K, Takagi J, Sato J, Shimizu H, Saiki H, Hoshiai M, Ichida F, Takeda S, Takigiku K, Inamura N, Kajino H, Murakami T, Shimizu W, Horie M.	Clinical characteristics and genetic background of congenital long QT syndrome diagnosed in fetal, neonatal and infantile life. A nation-wide questionnaire survey in Japan.	Circ Arrhythm Electrophysiol.	3	10-17	2010

堀江　稔	デスモゾーム病としての不整脈源性右室心筋症－デスモゾーム分子遺伝子異常	医学のあゆみ	232	588-592	2010
伊藤　英樹，堀江　稔	遺伝子異常と不整脈	臨床と研究	87	98-101	2010
伊藤　英樹，堀江　稔	QTが長ければQT延長症候群か？	medicina	47	66-68	2010
Wu J, Shimizu W, Ding W-G, Ohno S, Toyada F, Itoh H, Zang W-J, Miyamoto Y, Kamakura S, Matsuura H, Nademanee J, Brugada J, Brugada P, Brugada R, Vatta M, Towbin JA, Antzelevitch C, Horie M.	KCNE2 modulation of KV4.3 current and its potential role in fatal rhythm disorders.	Heart Rhythm	7	199-205	2010
Ikrar T, Hanawa H, Watanabe H, Aizawa Y, Ramadan MM, Chinushi M, Horie M, Aizawa Y	Evaluation of channel function after alteration of amino acid residues at the pore center of KCNQ1 channel.	BBRC	378	589-594	2009
Zankov DP, Yoshida H, Tsuji K, Toyoda F, Ding WG, Matsuura H, Horie M	Adrenergic regulation of the rapid component of delayed rectifier K^+ current: Implications for arrhythmogenesis in LQT2 patients.	Heart Rhythm	6	1038-1046	2009
Itoh H, Yamamoto T, Sugihara H, Saotome T, Eguchi Y, Asai T, Horie M	Aortopulmonary artery dissection.	JACC	54	1990	2009
Nakazawa Y, Ashihara T, Tsutamoto T, Ito M, Horie M	Endothelin-1 as a predictor of atrial fibrillation recurrence after pulmonary vein isolation.	Heart Rhythm	6	725-730	2009
Ogawa S, Yamashita T, Yamazaki T, Aizawa Y, Atarashi H, Inoue H, Ohe T, Ohtsu H, Okumura K, Katoh T, Kamakura S, Kumagai K, Kurachi Y, Kodama I, Koretsune Y, Saikawa T, Sakurai M, Sugi K, Tabuchi T, Nakaya H, Nakayama T, Hirai M, Fukatani M, Mitamura H; J-RHYTHM Investigators	Optimal treatment strategy for patients with paroxysmal atrial fibrillation: J-RHYTHM Study	Circulation Journal	73	242-248	2009
Zankov DP, Toyoda F, Omatsu-Kanbe M, Matsuura M, Horie M	Angiotensin II type 1 receptor mediates partially hyposmotic-induced increase of IKs current in guinea pig atrium.	Pflugers Arch.	458	837-849	2009
Nishio Y, Makiyama T, Itoh H, Sakaguchi T, Ohno S, Gong Y-Z, Yamamoto S, Ozawa T, Ding W-G, Toyoda F, Kawamura M, Akao M, Matsuura H, Kita T, Horie M	D85N, a KCNE1 polymorphism, is a disease-causing gene variant in long QT syndrome.	JACC	54	812-819	2009

Tamaki S, Nakamura Y, Tabara Y, Okamura T, Kanda H, Kita Y, Kadowaki T, Tsujita Y, Turin T C, Horie M, Miki T, Ueshima H.	Association between polymorphism of the AGTR1 and cardiovascular events in a Japanese general sample (The Shigaraki Study)	Int J Cardiol	136	354-355	2009
Inoue H, Fujiki A, Origasa H, Ogawa S, Okumura K, Kubota I, Aizawa Y, Yamashita T, Atarashi H, Horie M, Ohe T, Doi Y, Shimizu A, Chishaki A, Saikawa T, Yano K, Kitabatake A, Mitamura H, Kodama I, Kamakura S.	Prevalence of atrial fibrillation in the general population of Japan:An analysis based on periodic health examination.	Int J Cardiol	137	102-107	2009
Okamura T, Sekikawa A, Kadowaki T, El-Saed A, Abbott DR, Curb JD, Edmundowicz D, Nakamura Y, Murata K, Kashiwagi A, Kim ST, Evans RW, Zmuda JM, Maegawa H, Hozawa A, Mitsunami K, Nisio Y, Iva MG, Horie M, Miyamastu N, Murakami Y, Kuller LH,Ueshima H.	Cholesteryl ester transfer protein, coronary calcium and intima-media thickness of the carotid artery in middle-aged Japanese men.	Am J Cardiol.	104	818-822	2009
Kamakura S, Ohe T, Nakazawa K, Aizawa Y, Shimizu A, Horie M, Ogawa S, Okumura K, Tsuchihashi K, Sugi K, Makita N, Hagiwara N, Inoue H, Atarashi H, Aihara N, Shimizu W, Kurita T, Suyama K, Noda T, Satomi K, Okamura H, Tomoike H.	Long-term prognosis of probands with brugada-pattern ST-Elevation in leads V1-V3.	Circulation Arrhythmia & EP	2	495-503	2009
Itoh H, Sakaguchi T, Ding WS, Watanabe E, Watanabe I, Nishio Y, Makiyama T, Ohno S, Akao M, Higashi Y, Zenda N, Kubota T, Mori C, Okajima K, Haruna T, Miyamoto A, Kawamura M, Ishida K, Nagaoka I, Oka Y, Nakazawa Y, Yao T, Jo H, Sugimoto Y, Ashihara T, Hayashi H, Ito M, Imoto K, Matsuura H, Horie M	Latent genetic backgrounds and molecular pathogenesis in drug-induced long QT syndrome.	Circulation Arrhythmia & EP	2	511-523	2009
Wu J, Ding WG, Matsuura H, Tsuji K, Zang WJ, Horie M.	Inhibitory actions of LY294002,a phosphatidylinositol 3-kinase inhibitor,on the human Kv1.5 channel.	Brit J Pharm	56	377-387	2009

Ohno S, Toyoda F, Zankov D, Yoshida H, Makiyama T, Tsuji K, Honda T, Obayashi K, Matsuura H, Shimizu W, Miyamoto Y, Kamakura S, Kita T, Horie M.	Novel KCNE3 mutations interact with KCNQ1 and cause long QT syndrome.	Human Mutation	30	557-563	2009
Itoh H, Sakaguchi T, Ashihara T, Ding G W, Nagaoka I, Oka Y, Nakazawa Y, Yao T, Jo H, Ito M, Matsuura H, Horie M.	A novel KCNH2 mutation as a modifier for short QT interval.	Int J Cardiol.	137	83-85	2009
Inoue H, Fujiki A, Origasa H, Ogawa S, Okumura K, Kubota I, Aizawa Y, Yamashita T, Atarashi H, Horie M, Ohe T, Doi Y, Shimizu A, Chishaki A, Saikawa T, Yano K, Kitabatake A, Mitamura H, Kodama I, Kamakura S.	Prevalence of atrial fibrillation in the general population of Japan: an analysis based on periodic health examination.	Int J Cardiol.	137	102-107	2009
堀江　稔	薬剤性QT延長症候群.	ICUとCCU	33	19-24	2009
堀江　稔	Arrhythmias and sudden death in heart failure.	AHA Highlights 2008		136-140	2009
牧山　武，赤尾　昌治，堀江　稔	遺伝子変異と多型	Brugada症候群－病態解明から診断・治療指針の決定－		210-223	2009
堀江　稔	TOP-不整脈研究の流れ.	BIO Clinica	24	405-405	2009
堀江　稔	Romano-Ward症候群.	小児科診療	72	221	2009
堀江　稔	Jervell lange Nielsen.	小児科診療	72	215	2009
堀江　稔	Andersen症候群.	Current Therapy	27	458-459	2009
堀江　稔	アップストリーム治療	診断と治療	97	1022-1027	2009
堀江　稔	薬剤性QT延長症候群	循環器科	65	546-550	2009
堀江　稔	不整脈研究の流れ	BIO Clinica	310	405	2009
本荘　晴明，山崎　正俊，石黒　有子，神谷香一郎，佐久間一郎，芦原　貴司，堀江　稔，児玉　逸雄	Optical mappingによるspiral waveの解析.	心電図	29	231-235	2009
堀江　稔	QT延長症候群.	小児科	50	1083-1087	2009
堀江　稔	遺伝性不整脈	Heart View	13	47-51	2009
堀江　稔	致死性不整脈に関する遺伝子研究の現状	不整脈 News & Views		8-10	2009
西尾由貴子，堀江　稔	QT延長の潜在的危険性の予知－遺伝子多型：KCNE1-D85N－.	循環器専門医	17	237-242	2009

Ⅳ. 研究成果の刊行物・別刷

Journal of the American College of Cardiology
© 2009 by the American College of Cardiology Foundation
Published by Elsevier Inc.

Vol. 54, No. 9, 2009
ISSN 0735-1097/09/$36.00
doi:10.1016/j.jacc.2009.06.005

QUARTERLY FOCUS ISSUE: HEART RHYTHM DISORDERS

D85N, a KCNE1 Polymorphism, Is a Disease-Causing Gene Variant in Long QT Syndrome

Yukiko Nishio, MD,* Takeru Makiyama, MD, PHD,* Hideki Itoh, MD, PHD,† Tomoko Sakaguchi, MD, PHD,† Seiko Ohno, MD, PHD,* Yin-Zhi Gong, MD, PHD,† Satoshi Yamamoto, MD,§ Tomoya Ozawa, MD, PHD,† Wei-Guang Ding, MD, PHD,‡ Futoshi Toyoda, PHD,‡ Mihoko Kawamura, MD,† Masaharu Akao, MD, PHD,* Hiroshi Matsuura, MD, PHD,‡ Takeshi Kimura, MD, PHD,* Toru Kita, MD, PHD,* Minoru Horie, MD, PHD†

Kyoto, Shiga, and Osaka, Japan

Objectives This study aims to address whether D85N, a KCNE1 polymorphism, is a gene variant that causes long QT syndrome (LQTS) phenotype.

Background KCNE1 encodes the beta-subunit of cardiac voltage-gated K^+ channels and causes LQTS, which is characterized by the prolongation of the QT interval and torsades de pointes, a lethal arrhythmia. D85N, a KCNE1 polymorphism, is known to be a functional variant associated with drug-induced LQTS.

Methods In order to elucidate the prevalence and clinical significance of this polymorphism, we performed genetic screening in 317 LQTS probands. For comparison, we examined its presence in 496 healthy control subjects. We also conducted biophysical assays for the D85N variant in mammalian cells.

Results The allele frequency for D85N carriers was 0.81% in healthy people. In contrast, among LQTS probands, there were 1 homozygous and 23 heterozygous carriers (allele frequency 3.9%). Seven of 23 heterozygous carriers had additional mutations in LQTS-related genes, and 3 female subjects had documented factors predisposing to the symptom. After excluding these probands, the D85N prevalence was significantly higher compared with control subjects (allele frequency 2.1%, $p < 0.05$). In a heterologous expression study with Chinese hamster ovarian cells, KCNE1-D85N was found to exert significant loss-of-function effects on both KCNQ1- and KCNH2-encoded channel currents.

Conclusions The KCNE1-D85N polymorphism was significantly more frequent in our LQTS probands. The functional variant is a disease-causing gene variant of LQTS phenotype that functions by interacting with KCNH2 and KCNQ1. Since its allele frequency was ~1% among control individuals, KCNE1-D85N may be a clinically important genetic variant. (J Am Coll Cardiol 2009;54:812–9) © 2009 by the American College of Cardiology Foundation

Long QT syndrome (LQTS) is a disorder that is characterized by repolarization abnormalities in the heart, leading to torsades de pointes (TdP), syncope, and sudden death. Among the LQTS-related genes identified to date, KCNQ1 and KCNE1 are known to encode the alpha and beta subunits of voltage-gated K^+ channels, which carry I_{Ks}, a slowly activating component of delayed rectifier K^+ current (1,2). KCNE1 is also known to regulate KCNH2 (3), which encodes the Kv11.1 protein, the alpha subunit of rapidly activating delayed rectifier K^+ current (I_{Kr}) (4–6).

See page 820

A KCNE1 C-terminal polymorphism, D85N, has been found in the normal population and is known to cause a G-to-A transition at codon 253 (c.253G>A), which leads to the amino acid substitution of aspartic acid for asparagines (7). This has been shown to cause an approximately 50% reduction in KCNQ1-encoded currents in a heterologous expression system using *Xenopus* oocytes (8), although biophysical study data are not available for mammalian cells.

From the *Department of Cardiovascular Medicine, Kyoto University Graduate School of Medicine, Kyoto, Japan; Departments of †Cardiovascular and Respiratory Medicine and ‡Physiology, Shiga University of Medical Science, Shiga, Japan; and the §Third Department of Internal Medicine, Osaka Medical College, Osaka, Japan.
This work was supported by Grants-in-Aid in Scientific Research from the Ministry of Education, Culture, Science, and Technology of Japan, and a Health Sciences Research Grant (H18-Research on Human Genome-002) from the Ministry of Health, Labor, and Welfare of Japan.

Manuscript received September 8, 2008; revised manuscript received May 21, 2009, accepted June 15, 2009.

The allele frequency of the polymorphism is reported to be 0.7% in apparently healthy Asians (7). Paulussen et al. (9) demonstrated in a European population that the allele frequency of D85N was 5% in acquired LQTS patients who experienced TdP as a result of drug administration, but was 0% in the control group. Iwasa et al. (10) reported that the allele frequency was 2% in 100 Japanese cases, but their cohort contained both LQTS patients and normal individuals.

In the present study, we examined the incidence rate of KCNE1-D85N polymorphisms in 317 LQTS probands from unrelated families and 496 control healthy individuals. We identified 23 heterozygous and 1 homozygous probands (allele frequency 3.9%), described the demographics of these index patients, and examined the possibility that the D85N polymorphism is an LQTS-causing genetic variant. We also conducted detailed functional assays of the variant while it was coexpressed with the 2 alpha subunits of cardiac delayed rectifier K^+ channels, KCNQ1 and KCNH2, by using a heterologous expression system involving Chinese hamster ovarian (CHO) cells.

Methods

Study subjects. Three hundred and seventeen consecutive LQTS probands who showed a prolongation of the QT interval were referred to our laboratory for genetic evaluation and were enrolled in our analysis. The electrocardiogram diagnostic criteria of Keating and Sanguinetti (11) included a corrected QT interval (QTc) of ≥470 ms in asymptomatic individuals and a QTc of >440 ms for male subjects and of >460 ms for female subjects that had 1 or more of the following: 1) stress-related syncope; 2) documented TdP; or 3) a family history of early sudden cardiac death.

The protocol for genetic analysis was approved by our institutional ethics committee and was performed under its guidelines. Informed consent was obtained from all individuals or their guardians before the analysis. The QT intervals were measured from electrocardiographic lead II or an available rhythm strip and were corrected for heart rate according to Bazett's formula. As for the control cohort, we screened the frequency of the D85N polymorphism in 496 randomly selected cases, consisting of healthy volunteers and mutation-negative family members such as probands' spouses. Their QTc were <440 ms for male subjects and <460 ms for female subjects.

Genotyping. Genomic deoxyribonucleic acid (DNA) was isolated from venous blood by use of the QIAamp DNA midikit (Qiagen, Hilden, Germany). Genetic screening for KCNE1-D85N was performed by direct polymerase chain reaction. Other LQTS-related genes, including KCNQ1, KCNH2, SCN5A, KCNE1, KCNE2, and KCNJ2, were assayed by denaturing high-performance liquid chromatography using a WAVE System Model 3500 (Transgenomic, Omaha, Nebraska). Abnormal conformers were amplified by polymerase chain reaction. Sequencing was performed with an ABI PRISM3100 DNA sequencer (Applied Biosystems, Wellesley, Massachusetts).

Abbreviations and Acronyms

CHO = Chinese hamster ovarian
LQTS = long QT syndrome
QTc = corrected QT interval
TdP = torsades de pointes

Site-directed mutagenesis. Complementary deoxyribonucleic acid (cDNA) for human KCNQ1 (GenBank AF000571) and KCNE1 (GenBank M26685) were kindly provided by Dr. J. Barhanin (Institut de Pharmacologie Moléculaire et Cellulaire, CNRS, Valbonne, France). The cDNAs were subcloned into pIRES2-EGFP (for KCNQ1) and pIRES-CD8 (for both wild-type and mutated KCNE1) vectors. cDNA for human KCNH2 (GenBank AF363636) was kindly donated by Dr. M. Sanguinetti (University of Utah, Salt Lake City, Utah). The cDNA was subcloned into a pRc-CMV vector. A KCNE1-D85N variant was constructed using a Quick Change II XL Site-Directed Mutagenesis Kit, according to the manufacturer's instructions (Stratagene, La Jolla, California). Nucleotide sequence analysis was performed on each variant construct before the expression study to confirm their sequences.

Cell transfection. CHO cells were maintained at 37°C in Dulbecco's modified Eagle medium and Ham's F12 nutritional mixture (Gibco-BRL, Rockville, Maryland) containing 10% fetal bovine serum supplemented with 1% penicillin and 1% streptomycin. Wild-type KCNQ1, KCNH2, and wild-type and/or variant KCNE1 clones were expressed transiently in CHO cells using the LipofectAMINE method according to the manufacturer's instructions (Invitrogen, Carlsbad, California).

To identify the cells that were positive for KCNH2 expression, CHO cells were cotransfected with 1 μg of pRc-CMV/KCNH2 vector and 0.5 μg of pEGFP-N1/CMV vector. Forty-eight to 72 h after transfection, green fluorescent protein-positive cells and anti-CD8 antibody-coated bead (Dynabeads CD8, Dynal Biotech, Oslo, Norway) decorated cells were used for the patch-clamp study.

Electrophysiological assays. Whole-cell configuration of patch-clamp techniques was employed to record membrane currents at 37°C with an EPC-8 patch-clamp amplifier (HEKA, Lambrecht, Germany). Pipette resistance ranged from 2.5 to 4 MΩ when filled with the pipette solutions described in the following text. The series resistance was electronically compensated for at 70% to 85%. The extracellular solution contained (mmol/l): 140 NaCl, 0.33 NaH_2PO_4, 5.4 KCl, 1.8 $CaCl_2$, 0.5 $MgCl_2$, 5.5 glucose, and 5 HEPES, and the pH was adjusted to 7.4 with NaOH. The internal (pipette) solution contained (mmol/l): 70 potassium aspartate, 70 KOH, 40 KCl, 10 KH_2PO_4, 1 Mg_2SO_4, 3 Na_2-ATP, 0.1 Li_2-GTP, 5 EGTA, and 5 HEPES, and the pH was adjusted to 7.2 with KOH.

KCNQ1/KCNE1-encoded currents were measured by depolarizing pulses from a holding potential of −90 mV to test potentials between −70 and +50 mV (with a 10-mV step increment), before being repolarized to −50 mV in

order to monitor tail current amplitude. KCNH2/KCNE1-encoded currents were elicited by depolarizing pulses from a holding potential of −80 mV to test potentials between −60 to +50 mV (with a 10-mV step increment), before being repolarized to −60 mV in order to monitor tail current amplitude. Current densities (pA/pF) were calculated for each cell studied, by normalizing peak tail current amplitude to cell capacitance (Cm). The Cm was calculated by fitting a single exponential function to the decay phase of the transient capacitive current in response to ± 5 mV voltage steps (20 ms) from a holding potential of −50 mV. The liquid junction potential between the test solution and the pipette solution was measured as approximately −10 mV and was corrected. Data were collected and analyzed using the Patch master and Igor Pro (WaveMetrics, Lake Oswego, Oregon).

Data analyses. The voltage-dependence of current activation was determined by fitting the normalized tail current (Itail) versus test potential (Vtest) to Boltzmann's function, which is expressed by: Itail = $1/(1 + \exp[(V_{0.5} - Vt)/k])$, where $V_{0.5}$ is the voltage at which the current is half-activated and k is the slope factor. Time constants for deactivation (τ_{fast} and τ_{slow}) were obtained by fitting a 2-exponential function to the time course of the deactivating tail currents. All data are expressed as mean ± standard error. Statistical comparisons were made using analysis of variance, followed by a *t* test, and differences were considered significant at a value of $p < 0.05$.

Results

Clinical characteristics and genotyping. Of the 496 control volunteers, 8 (mean QTc 420.5 ± 7.5 ms) had heterozygous D85N genotypes (allele frequency 0.81%). In contrast, 23 of the 317 LQTS probands had heterozygous D85N genotypes and 1 (Table 1) (Patient #24) had a homozygous D85N genotype (allele frequency 3.9%). Table 1 and Figure 1 summarize the demographics of the 24 index patients. Their mean age was 34.8 ± 4.4 years, and their mean QTc was 507.9 ± 9.2 ms. Among the D85N-negative cases, we identified 116 probands that were positive for other LQTS-related gene mutations (Fig. 1), and their mean QTc was significantly longer (540.6 ± 6.1 ms) than those of the 24 D85N carriers ($p < 0.05$).

Seven of the 23 heterozygous probands (30%) had other LQTS-related gene variants (KCNQ1 or KCNH2), and 3 female patients (13%; Patients #1, #6, and #10) had documented predisposing factors, such as electrolyte disturbances, QT prolonging drug intake, or bradycardia (Table 1). The allele frequency of the remaining 13 patients (2.1%) was significantly higher than that in the control subjects ($p < 0.05$). Six of these 13 patients (46%) had syncope and/or TdP while 9 of 10 patients (90%) with multiple genetic variants or triggering factors were symptomatic (Fig. 1).

The mean onset age of the 6 symptomatic heterozygous D85N carriers without compromised factors to affect QT

Table 1 Clinical Characteristics of the LQTS Probands Who Carried the KCNE1-D85N Variant

Patient #	Age (F/M)	QTc (ms)	Syncope	TdP	Compound Variant	Underlying Predisposing Triggers
1	36 (F)	540	+	+		Drug (bromocriptine), hypokalemia
2	9 (M)	478	–	–		
3	21 (F)	533	–	+	KCNH2 (a, S706F)*	Drug (amphetamine), hypokalemia
4	42 (F)	650	+	+		
5	51 (F)	490	+	+	KCNH2 (a, E58K)	Sinus bradycardia
6	73 (F)	493	+	–		Drug (disopyramide), sinus bradycardia
7	30 (F)	502	+	–	KCNH2 (G745fs+55X)*	
8	17 (F)	470	–	–		
9	13 (F)	462	+	–	KCNH2 (a, S320L)	
10	41 (F)	490	–	+		Hypomagnesemia
11	73 (F)	608	+	–	KCNQ1 (a, S277L)	Sinus bradycardia
12	75 (F)	494	+	+		
13	17 (M)	500	–	–		
14	13 (F)	512	+	–		
15	57 (M)	472	–	–		
16	53 (M)	462	+	+		
17	17 (F)	520	+	–		
18	22 (F)	472	–	–		
19	13 (F)	522	–	–	KCNH2 (a, R823W)	
20	13 (M)	467	+	–		
21	52 (M)	524	+	+	KCNH2 (a, R948S)*	Drug (minor tranquilizer), hypokalemia
22	11 (M)	491	–	–		
23	51 (M)	493	–	–		
24	39 (F)	545	–	–		

*Novel variant.
LQTS = long QT syndrome; QTc = corrected QT interval; TdP = torsades de pointes.

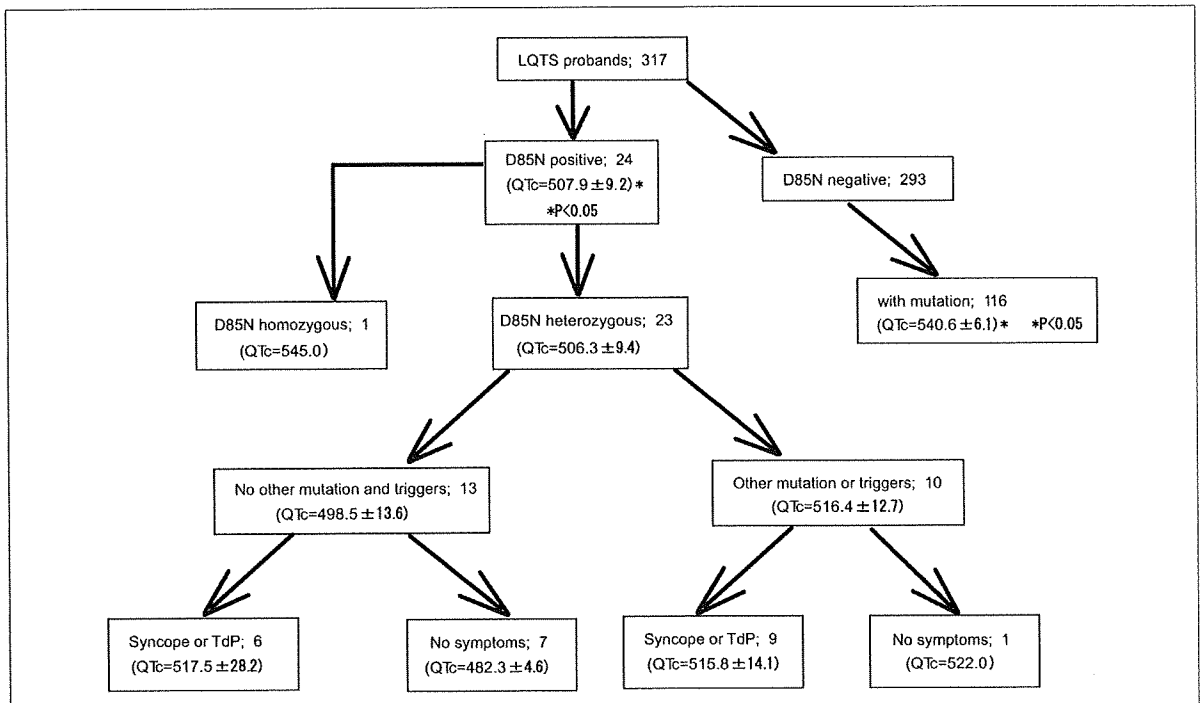

Figure 1 Summary of LQTS Probands

LQTS = long QT syndrome; QTc = corrected QT interval; TdP = torsades de pointes.

interval was 35.5 ± 10.4 years. It was significantly older than the mean onset age of the other genotyped symptomatic LQTS patients (21.0 years in our cohort of 94 genotyped LQTS) (Horie M. et al., unpublished data, September 2008). Although the clinical features of KCNE1-D85N–positive probands differed with respect to the QTc and the onset age from those of other genotyped LQTS patients, this variant appeared to be a disease-causing gene variant in congenital LQTS.

Biophysical assays of the genetic variant. KCNE1-D85N WITH KCNQ1. In order to confirm that the D85N is a disease-causing variant, we conducted functional assays using a heterologous expression system with a mammalian cell line (CHO cells). In the first line of experiments, we examined how KCNE1-D85N affected the reconstituted KCNQ1/KCNE1 currents. Figure 2 depicts representative current traces recorded from cells that coexpressed KCNQ1 and wild-type (Fig. 2A-a) or D85N (Fig. 2A-b) KCNE1 (1 μg each). Peak tail current densities measured after repolarization to −50 mV from various test pulses were calculated in individual cells and are plotted as a function of test potential in Figure 2B. Solid circles indicate the mean peak current densities from 21 cells that were transfected with KCNQ1 and wild-type KCNE1; open circles indicate the mean peak current densities from 25 cells that were transfected with KCNQ1 and D85N, and solid triangles indicate the mean peak current densities from 25 cells that were transfected with KCNQ1 alone. D85N reduced the peak tail currents of wild-type KCNQ1/KCNE1-encoded currents by 28% at 0 mV test potential ($p < 0.05$ vs. wild type).

In Figure 2C, peak tail current densities have been normalized using the current densities recorded after a test pulse to +50 mV and are plotted as a function of test potential. Fitting of data plots to Boltzmann's equation yielded $V_{0.5}$ values of −4.36 ± 1.8 mV for the wild type and 0.38 ± 1.7 mV for D85N ($p < 0.05$), suggesting that the KCNE1 variant produced a significantly positive shift in KCNQ1-encoded current activation kinetics (Table 2). The deactivation process of tail currents could be fitted by 2 exponentials, yielding fast and slow time constants. No significant difference with respect to the fast time constants was evident between the wild-type and D85N genotypes; however, slow deactivation was significantly accelerated by coexpression of D85N (Table 2).

KCNE1-D85N WITH KCNH2. In the next line of experiments, we examined how KCNE1 and its D85N variant influence KCNH2-encoded currents. Figures 3A-a and 3A-b depict 2 sets of current traces recorded from CHO cells that had been transfected with KCNH2 plus wild-type or D85N KCNE1 (1 μg each). Peak tail current densities at −60 mV were calculated in the respective cells and are plotted as a function of test potential in Figure 3B. Solid circles and open circles indicate the mean current densities calculated from 23

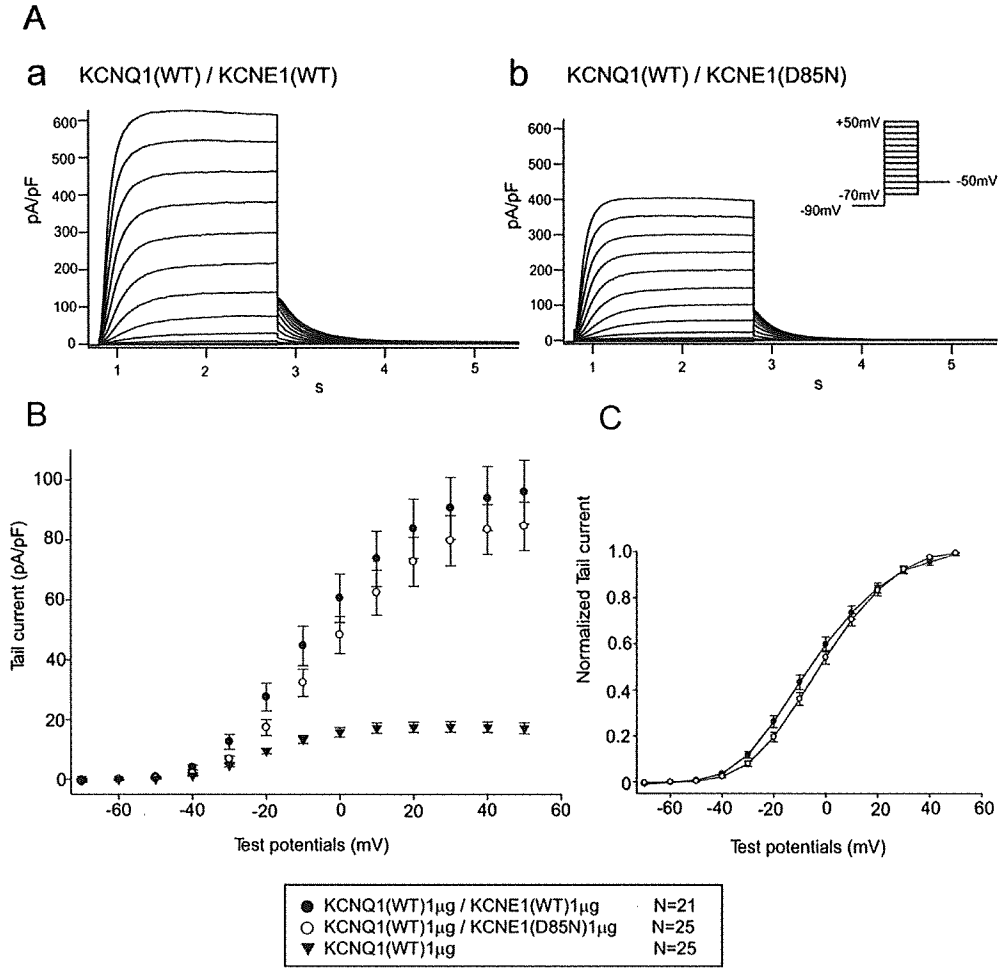

Figure 2 **Functional Expression of KCNQ1 With KCNE1-D85N in Chinese Hamster Ovarian Cells**

(A) Representative current traces of KCNQ1 coexpression with the wild-type (WT) or D85N KCNE1. **(a)** KCNQ1 (1 μg) plus WT KCNE1 (1 μg). **(b)** KCNQ1 (1 μg) plus D85N KCNE1 (1 μg). **(B and C)** Functional consequences of KCNQ1 coexpression with the WT or D85N KCNE1 (**[B]** activation curve; **[C]** normalized activation curve). **Solid circles** indicate the mean peak current densities from 21 cells that have been transfected with KCNQ1 and WT KCNE1 (1 μg of each), and **open circles** indicate the mean peak current densities from 25 cells that have been transfected with KCNQ1 and D85N KCNE1 (1 μg of each). **Solid triangles** show those obtained from 25 cells that were transfected with KCNQ1 alone (1 μg).

and 20 cells, respectively, which were transfected with 1 μg of KCNH2 and 1 μg of wild-type or D85N KCNE1.

D85N reduced the peak tail currents of wild-type KCNH2/KCNE1-encoded currents by 31% to 36% at test potentials between 0 and +50 mV ($p < 0.005$ vs. wild type). Fitting of normalized data to Boltzmann's equation yielded a $V_{0.5}$ of −18.33 ± 0.8 mV for the wild-type KCNH2/KCNE1 and of −22.07 ± 1.6 mV for KCNH2/KCNE1-D85N ($p < 0.05$), suggesting that the KCNE1 variant causes a significantly negative shift of KCNH2/KCNE1-encoded current activation kinetics (Fig. 3C, Table 2). Deactivation of tail currents could be fitted by 2 exponentials, yielding fast and slow time constants. The fast and slow kinetics were not significantly different between the 2 types of KCNH2 channel currents (Table 2).

Discussion

The present study demonstrates that the allele frequency of KCNE1-D85N is significantly higher in LQTS patients than in control subjects after excluding cases with compromised factors to prolong QT interval ($p < 0.05$). A biophysical assay of D85N showed that the variant affected both reconstituted I_{Ks} and I_{Kr} channel function, leading to a prolongation of the QTc with D85N working as a disease-causing variant. In a heterologous expression system with *Xenopus* oocytes (8),

Table 2 $V_{0.5}$, Slope Factor k, and τ Deactivation at +20 mV

	n	$V_{0.5}$	k	τ_{fast}	τ_{slow}
KCNQ1 (WT) 1 μg	25	−20.86 ± 1.034	8.223 ± 0.421	0.070 ± 0.005	0.136 ± 0.019
KCNQ1 (WT) 1 μg/KCNE1 (WT) 1 μg	21	−4.364 ± 1.834*	12.724 ± 0.407*	0.145 ± 0.013*	0.586 ± 0.070†
KCNQ1 (WT) 1 μg/KCNE1 (D85N) 1 μg	25	0.382 ± 1.717*‡	12.566 ± 0.429*	0.141 ± 0.013*	0.409 ± 0.050*‡
KCNH2 (WT) 1 μg/KCNE1 (WT) 1 μg	23	−18.326 ± 0.775	7.373 ± 0.289	0.183 ± 0.016	1.077 ± 0.102
KCNH2 (WT) 1 μg/KCNE1 (D85N) 1 μg	20	−22.069 ± 1.560§	7.037 ± 0.389	0.193 ± 0.013	1.258 ± 0.090

*$p < 0.0001$ versus KCNQ1 (wild type [WT]) 1 μg; †$p = 0.0001$ versus KCNQ1 (WT) 1 μg; ‡$p < 0.05$ versus KCNQ1 (WT) 1 μg/KCNE1 (WT) 1 μg; §$p < 0.05$ versus KCNH2 (WT) 1 μg/KCNE1 (WT) 1 μg.

KCNE1-D85N has been reported to cause an approximately 50% reduction in KCNQ1-encoded currents, although data for mammalian cells is not available. In our experiments using CHO cells, D85N significantly reduced KCNQ1-encoded currents by 28% ($p < 0.05$ vs. wild type), although this effect was smaller than that in *Xenopus* oocytes.

When KCNH2 was coexpressed with the wild-type or D85N variant of KCNE1, D85N significantly reduced wild-type KCNH2/KCNE1-encoded currents by 31% to 36% ($p < 0.005$ vs. wild type). Regarding the interaction between KCNE1 and KCNH2, McDonald et al. (3) demonstrated that KCNE1 forms a stable complex with KCNH2 and

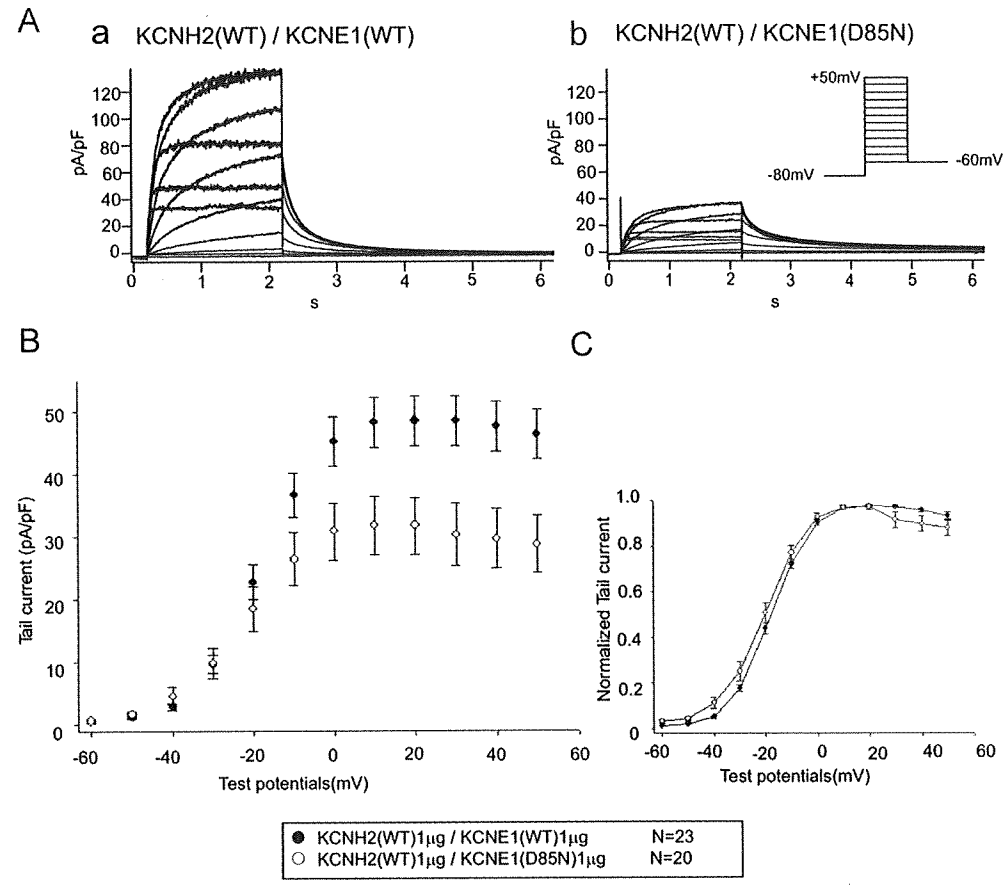

Figure 3 Functional Expression of KCNH2 With KCNE1-D85N in Chinese Hamster Ovarian Cells

(A) Representative current traces of KCNH2 coexpression with the wild-type (WT) or D85N KCNE1. **(a)** KCNH2 (1 μg) plus WT KCNE1 (1 μg). **(b)** KCNH2 (1 μg) plus D85N KCNE1 (1 μg). **(B and C)** Functional consequences of KCNH2 coexpression with the WT or D85N of KCNE1 **([B]** activation curve; **[C]** normalized activation curve). **Solid circles** indicate data from 23 cells that were transfected with KCNH2 and WT KCNE1 (1 μg of each). **Open circles** indicate data from 20 cells that were transfected with KCNH2 and D85N KCNE1 (1 μg of each).

up-regulates I_{Kr}-like currents by 50% in CHO cells. Bianchi et al. (12) also showed interactions between the KCNE1-D76N mutation and both KCNQ1 and KCNH2 in HEK cells. In atrial tumor myocytes that expressed I_{Kr} alone, Yang et al. (13) demonstrated that antisense oligonucleotides against minK cDNA (KCNE1) significantly reduced the I_{Kr} by ~62%. More recently, Ohno et al. (14) identified a missense KCNE1 mutation, A8V, in a sporadic case of LQTS and reported that the mutation significantly reduced the magnitude of KCNH2- but not KCNQ1-encoded currents.

Collectively, it is of clinical importance that the KCNE1-D85N variant modifies not only KCNQ1- but also KCNH2-coded channel currents. Furthermore, its inhibitory action on KCNH2 was even stronger than that on KCNQ1. The KCNE1-D85N polymorphism may therefore cause phenotypes similar to those observed in type 2 LQTS such as bradycardia (15,16). The deactivation process of I_{Kr} plays a significant role in maintaining the appropriate rate of pacemakers (17) and, therefore, a decreased I_{Kr} will lead to sinus bradycardia. In the present study, 3 D85N carriers (13%) had sinus bradycardia (Table 1).

The mean onset age of 6 symptomatic heterozygous D85N carriers (Table 1) was 35.5 years, and this was significantly older than the mean age of other genotyped symptomatic LQTS patients. Shimizu et al. (18) reported that in 95 Japanese LQT1 patients with transmembrane domain mutations or C-terminal domain mutations, the mean ages of first event were 11 ± 8 years and 13 ± 9 years. Nagaoka et al. (19) also demonstrated that in 118 Japanese LQT2 patients with pore mutations or nonpore mutations, the mean ages of first event were 16 ± 10 years and 20 ± 13 years. In addition, the mean QTc of 13 D85N carriers was prolonged (498.5 ± 13.6 ms) but significantly shorter than that in 116 probands with other LQTS-related gene mutations (541 ms) (Fig. 1). These different phenotypes appear to reflect the fact that D85N causes a milder channel dysfunction than other LQTS mutations, and reveals a "forme fruste" phenotype (20).

The allele frequency of the KCNE1-D85N polymorphism was 0.81% among apparently healthy control individuals. We found only 1 report concerning D85N frequency (0.7%) (7) in control subjects, which showed equivalent results to our study. Based on 2008 healthy French individuals, Gouas et al. (21) demonstrated that the allele frequency of D85N was significantly higher in the 200 subjects with the longest QTc than in those with the shortest QTc (3.1% vs. 0.75%), suggesting that this single nucleotide polymorphism may influence the QTc length in healthy individuals.

LQTS can remain latent or subclinical because of "repolarization reserve" (22), and can become unmasked upon the intake of QT-prolonging drugs. Heterozygous D85N carriers in the control group may be at a potentially higher risk of long QT-related arrhythmias. Assuming that genetic surveys are feasible before drug therapy, D85N carriers may be recommended to avoid the secondary factors that predispose them to further QT prolongation such as QT prolonging drugs (23) and electrolyte disturbances (23–25). It is also clinically useful to search for other variants of long QT-related genes (8,26,27).

Study limitations. In the present study, we screened the mutations that are responsible for LQT1, 2, 3, 5, 6, and 7. Therefore, the comorbidity of other types of LQTS was not completely excluded, although their frequency was quite low. In general, single nucleotide polymorphisms are thought to be nonpathological although some may modify the clinical features of a disease. For example, the KCNH2-K897T polymorphism is a typical genetic modifier that aggravates LQTS phenotypes directly by reducing channel function in association with the KCNH2 mutation A1116V (28). Such a role for KCNE1-D85N was not addressed in this study and warrants further study.

Conclusions

KCNE1-D85N was a highly frequent variant in our LQTS probands and was found to cause loss-of-function effects on both I_{Kr} and I_{Ks} and work as a disease-causing variant. Since its allele frequency was 0.81% among control healthy individuals, KCNE1-D85N may be a clinically important genetic variant.

Acknowledgment

The authors are grateful to the Japanese long QT families for their willingness to participate in this study.

Reprint requests and correspondence: Dr. Minoru Horie, Department of Cardiovascular and Respiratory Medicine, Shiga University of Medical Science, Seta Tsukinowa-cho, Otsu, Shiga 520-2192, Japan. E-mail: horie@belle.shiga-med.ac.jp.

REFERENCES

1. Sanguinetti MC, Curran ME, Zou A, et al. Coassembly of K(V) LQT1 and minK(IsK) proteins to form cardiac I(Ks) potassium channel. Nature 1996;384:80–3.
2. Barhanin J, Lesage F, Guillemare E, Fink M, Lazdunski M, Romey G. K(V)LQT1 and IsK(minK) proteins associate to form the I(Ks) cardiac potassium current. Nature 1996;84:78–80.
3. McDonald TV, Yu Z, Ming Z, et al. A minK-HERG complex regulates the cardiac potassium current $I_{(Kr)}$. Nature 1997;388: 289–92.
4. Sanguinetti MC, Jiang C, Curran ME, Keating MT. A mechanistic link between an inherited and an acquired cardiac arrhythmia: HERG encodes the I_{Kr} potassium channel. Cell 1995;81:299–307.
5. Trudeau MC, Warmke JW, Ganetzky B, Robertson GA. HERG, a human inward rectifier in the voltage-gated potassium channel family. Science 1995;269:92–5.
6. Sanguinetti MC, Curran ME, Spector PS, Keating MT. Spectrum of HERG K^+-channel dysfunction in an inherited cardiac arrhythmia. Proc Natl Acad Sci U S A 1996;93:2208–12.
7. Ackerman MJ, Tester DJ, Jones GS, Will ML, Burrow CR, Curran ME. Ethnic differences in cardiac potassium channel variants: implications for genetic susceptibility to sudden cardiac death and genetic testing for congenital long QT syndrome. Mayo Clin Proc 2003;78: 1479–87.

8. Westenskow P, Splawski I, Timothy KW, Keating MT, Sanguinetti MC. Compound mutations: a common cause of severe long-QT syndrome. Circulation 2004;109:1834–41.
9. Paulussen AD, Gilissen RA, Armstrong M, et al. Genetic variations of KCNQ1, KCNH2, SCN5A, KCNE1, and KCNE2 in drug-induced long QT syndrome patients. J Mol Med 2004;82:182–8.
10. Iwasa H, Itoh T, Nagai R, Nakamura Y, Tanaka T. Twenty single nucleotide polymorphisms (SNPs) and their allelic frequencies in four genes that are responsible for familial long QT syndrome in the Japanese population. J Hum Genet 2000;45:182–3.
11. Keating MT, Sanguinetti MC. Molecular and cellular mechanisms of cardiac arrhythmias. Cell 2001;104:569–80.
12. Bianchi L, Shen Z, Dennis AT, et al. Cellular dysfunction of LQT5-minK mutants: abnormalities of I_{Ks}, I_{Kr} and trafficking in long QT syndrome. Hum Mol Genet 1999;8:1499–507.
13. Yang T, Kupershmidt S, Roden DM. Anti-minK antisense decreases the amplitude of the rapidly activating cardiac delayed rectifier K^+ current. Circ Res 1995;77:1246–53.
14. Ohno S, Zankov DP, Yoshida H, et al. N- and C-terminal KCNE1 mutations cause distinct phenotypes of long QT syndrome. Heart Rhythm 2007;4:332–40.
15. Zhang L, Timothy KW, Vincent GM, et al. Spectrum of ST-T-wave patterns and repolarization parameters in congenital long-QT syndrome: ECG findings identify genotypes. Circulation 2000;102: 2849–55.
16. Nemec J, Buncová M, Bůlková V, et al. Heart rate dependence of the QT interval duration: differences among congenital long QT syndrome subtypes. J Cardiovasc Electrophysiol 2004;15:550–6.
17. Ono K, Ito H. Role of rapidly activating delayed rectifier K+ current in sinoatrial node pacemaker activity. Am J Physiol 1995; 269:H453–62.
18. Shimizu W, Horie M, Ohno S, et al. Mutation site-specific differences in arrhythmic risk and sensitivity to sympathetic stimulation in the LQT1 form of congenital long QT syndrome: multicenter study in Japan. J Am Coll Cardiol 2004;44:117–25.
19. Nagaoka I, Shimizu W, Itoh H, et al. Mutation site dependent variability of cardiac events in Japanese LQT2 form of congenital long-QT syndrome. Cir J 2008;72:694–9.
20. Priori SG, Napolitano C, Schwartz PJ. Low penetrance in the long QT syndrome. Clinical impact. Circulation 1999;99:529–33.
21. Gouas L, Nicaud V, Berthet M, et al. Association of KCNQ1, KCNE1, KCNH2 and SCN5A polymorphisms with QTc interval length in a healthy population. Eur J Hum Genet 2005;13:1213–22.
22. Xiao L, Xiao J, Luo X, Lin H, Wang Z, Nattel S. Feedback remodeling of cardiac potassium current expression: a novel potential mechanism for control of repolarization reserve. Circulation 2008;118: 983–92.
23. Roden DM, Viswanathan PC. Genetics of acquired long QT syndrome. J Clin Invest 2005;115:2025–32.
24. Justo D, Prokhorov V, Heller K, Zeltser D. Torsade de pointes induced by psychotropic drugs and the prevalence of its risk factors. Acta Psychiatr Scand 2005;111:171–6.
25. Kusano KF, Hata Y, Yumoto A, Emori T, Sato T, Ohe T. Torsade de pointes with a normal QT interval associated with hypokalemia: a case report. Jpn Circ J 2001;65:757–60.
26. Schwartz PJ, Priori SG, Napolitano C. How really rare are rare diseases?: the intriguing case of independent compound mutations in the long QT syndrome. J Cardiovasc Electrophysiol 2003;14:1120–1.
27. Hsieh MH, Chen SA, Chiang CE, et al. Drug-induced torsades de pointes in one patient with congenital long QT syndrome. Int J Cardiol 1996;54:85–8.
28. Crotti L, Lundquist AL, Insolia R, et al. KCNH2-K897T is a genetic modifier of latent congenital long-QT syndrome. Circulation 2005; 112:1251–8.

Key Words: long QT syndrome ▪ single nucleotide polymorphism ▪ disease-causing variant.

Latent Genetic Backgrounds and Molecular Pathogenesis in Drug-Induced Long-QT Syndrome

Hideki Itoh, MD; Tomoko Sakaguchi, MD; Wei-Guang Ding, MD; Eiichi Watanabe, MD; Ichiro Watanabe, MD; Yukiko Nishio, MD; Takeru Makiyama, MD; Seiko Ohno, MD; Masaharu Akao, MD; Yukei Higashi, MD; Naoko Zenda, MD; Tomoki Kubota, MD; Chikara Mori, MD; Katsunori Okajima, MD; Tetsuya Haruna, MD; Akashi Miyamoto, MD; Mihoko Kawamura, MD; Katsuya Ishida, MD; Iori Nagaoka, MD; Yuko Oka, MD; Yuko Nakazawa, MD; Takenori Yao, MD; Hikari Jo, MD; Yoshihisa Sugimoto, MD; Takashi Ashihara, MD; Hideki Hayashi, MD; Makoto Ito, MD; Keiji Imoto, MD; Hiroshi Matsuura, MD; Minoru Horie, MD

Background—Drugs with I_{Kr}-blocking action cause secondary long-QT syndrome. Several cases have been associated with mutations of genes coding cardiac ion channels, but their frequency among patients affected by drug-induced long-QT syndrome (dLQTS) and the resultant molecular effects remain unknown.

Methods and Results—Genetic testing was carried out for long-QT syndrome–related genes in 20 subjects with dLQTS and 176 subjects with congenital long-QT syndrome (cLQTS); electrophysiological characteristics of dLQTS-associated mutations were analyzed using a heterologous expression system with Chinese hamster ovary cells together with a computer simulation model. The positive mutation rate in dLQTS was similar to cLQTS (dLQTS versus cLQTS, 8 of 20 [40%] versus 91 of 176 [52%] subjects, $P=0.32$). The incidence of mutations was higher in patients with torsades de pointes induced by nonantiarrhythmic drugs than by antiarrhythmic drugs (antiarrhythmic versus others, 3 of 14 [21%] versus 5 of 6 [83%] subjects, $P<0.05$). When reconstituted in Chinese hamster ovary cells, *KCNQ1* and *KCNH2* mutant channels showed complex gating defects without dominant negative effects or a relatively mild decreased current density. Drug sensitivity for mutant channels was similar to that of the wild-type channel. With the Luo-Rudy simulation model of action potentials, action potential durations of most mutant channels were between those of wild-type and cLQTS.

Conclusions—dLQTS had a similar positive mutation rate compared with cLQTS, whereas the functional changes of these mutations identified in dLQTS were mild. When I_{Kr}-blocking agents produce excessive QT prolongation (dLQTS), the underlying genetic background of the dLQTS subject should also be taken into consideration, as would be the case with cLQTS; dLQTS can be regarded as a latent form of long-QT syndrome. **(*Circ Arrhythmia Electrophysiol.* 2009;2:511-523.)**

Key Words: long-QT syndrome ■ secondary ■ drug ■ electrophysiology ■ ion channel

Congenital long-QT syndrome (cLQTS) is characterized by abnormally prolonged ventricular repolarization and familial inheritance, leading to polymorphic ventricular tachycardia (torsades de pointes [TdP]), causing sudden cardiac death.[1,2] In contrast, secondary long-QT syndrome can be induced by a variety of commercially available drugs, including antiarrhythmic drugs, antihistamines, antibiotics, and major tranquilizers.[3] In patients with drug-induced long-QT syndrome (dLQTS), after a washout period of the culprit drugs, the QT interval usually returns to within normal range. Genetic factors may underlie the susceptibility to drug-induced serious adverse reactions such as a long QT

Clinical Perspective on p 523

Received February 29, 2008; accepted July 6, 2009.

From the Department of Cardiovascular and Respiratory Medicine (H.I., T.S., A.M., M.K., K.I., I.N., Y.O., Y.N., T.Y., H.J., Y.S., T.A., H.H., M.I., M.H.) and the Department of Physiology (W.-G.D., H.M.), Shiga University of Medical Science, Shiga, Japan; the Department of Laboratory Medicine (E.W.), Fujita Health University School of Medicine, Toyoake, Japan; the Division of Cardiology (I.W.), Department of Medicine, Nihon University School of Medicine, Tokyo, Japan; the Department of Cardiovascular Medicine (Y.N., T.M., S.O., M.A.), Kyoto University Graduate School of Medicine, Kyoto, Japan; the Cardiovascular Division (Y.H., N.Z.), Showa University Fujigaoka Hospital, Yokohama, Japan; the Division of Cardiology (T.K.), Gifu University Graduate School of Medicine, Gifu, Japan; the Division of Cardiology (C.M.), Department of Internal Medicine, Jikei University School of Medicine, Daisan Hospital, Tokyo, Japan; the Department of Cardiology (K.O.), Hyogo Brain and Heart Center, Himeji, Japan; the Department of Cardiology (T.H.), Kitano Hospital, Osaka, Japan; and the Department of Information Physiology (K.I.), National Institute for Physiological Sciences, Okazaki, Japan.

The online-only Data Supplement is available at http://circep.ahajournals.org/cgi/content/full/CIRCEP.109.862649/DC1.

Correspondence to Minoru Horie, MD, Department of Cardiovascular and Respiratory Medicine, Shiga University of Medical Science, Seta-Tsukinowa, Otsu, Shiga, Japan 520-2192. E-mail horie@belle.shiga-med.ac.jp

Circ Arrhythmia Electrophysiol **is available at http://circep.ahajournals.org** **DOI: 10.1161/CIRCEP.109.862649**

interval and TdP. Sesti et al[4] demonstrated that a polymorphism of the *KCNE2* gene (T8A) is present in 1.6% of the population and is associated with drug-induced TdP related to quinidine and to sulfamethoxazole/trimethoprim administration. We have also previously reported that a mutant *SCN5A* channel (L1825P), found in an elderly woman with cisapride-induced TdP, appeared to have unique electrophysiological characteristics with both loss and gain of functions for the cardiac sodium current.[5] In addition, there have been several case reports with long-QT syndrome–associated gene mutations in dLQTS.[6–10] The accurate prevalence of long-QT syndrome–related gene mutations in a larger dLQTS cohort, however, remains unknown, and the relationship between genotypes and cellular electrophysiology has not been fully examined. The present study therefore aimed to survey mutations in long-QT syndrome–related genes responsible for dLQTS in 20 patients who had been referred to our institutes consecutively over the past 11 years and analyze the functional effects induced by these mutations.

Methods

Subjects

Blood samples of 305 subjects with long-QT syndrome, comprising 196 long-QT syndrome probands and 109 family members were referred to Kyoto University Graduate School of Medicine and Shiga University of Medical Sciences from March 1996 to January 2006 for genetic analysis. A diagnosis of dLQTS was made in those subjects who had not previously been diagnosed with long-QT syndrome and who only developed typical ECG features of QT prolongation after administration of culprit drugs. A diagnosis of cLQTS was made in those subjects with clinical phenotypes of long-QT syndrome, but without the involvement of secondary factors (eg, drugs, hypokalemia, or bradycardia). Among the subjects, 20 probands had drug-induced cardiac events (10.2% of long-QT syndrome probands). Their clinical information was collected, including family history of sudden death age 30 years or younger and long-QT syndrome members, previous syncope, ECGs, and serum electrolyte levels at the time of cardiac events. TdP was defined as either nonsustained or sustained ventricular tachycardia showing variation in the electronic polarity of the QRS complex and a "short-long-short" initiating sequence.[11] Written informed consent was obtained from all subjects in accordance with the guidelines approved by our institutional review board. QT intervals were measured in lead II or V_5, using the Bazett formula,[12] before and after allowing sufficient time for the complete washout of drugs.

Schwartz scores[13] were calculated in all probands. A Schwartz score ≧4 points indicates that long-QT syndrome is definitely present, a score of 2 or 3 points indicates there is a strong possibility that long-QT syndrome is present, whereas a score ≦1 point indicates a low probability of long-QT syndrome, respectively.[13]

Mutation Analysis

The protocol for genetic analysis was approved by and performed under the guidelines of the Institutional Ethics Committee at Shiga University of Medical Science. Genomic DNA was isolated from peripheral white blood cells using conventional methods. Genetic screening was performed for *KCNQ1, KCNH2, SCN5A, KCNE1, KCNE2,* and *KCNJ2,* using polymerase chain reaction/single-strand conformational polymorphism (PCR-DHPLC, WAVE system, Transgenomic Inc, Omaha, Neb) analysis.[14,15] For the abnormal DHPLC patterns, we determined the DNA sequences on both strands with an automated sequencer (PRISM 3130 Sequencer, Perkin Elmer, Calif).

Expression Plasmids

The expression plasmids pIRES2-EGFP/*KCNQ1*(wild type[WT]/*KCNQ1*) and pRc-CMV/*KCNH2* (wild-type [WT]/*KCNH2*) were kindly provided by Dr J. Barhanin (UMR 6097 CNRS and Université de Nice Sophia Antipolis, Valbonne, France) and Dr M. Sanguinetti (University of Utah, Salt Lake City, Utah), respectively. The mutations were introduced using overlap PCR. The mutant plasmids were constructed by substituting the 857-bp *Xho*I-*Bgl*II for R231C and R243H mutants, 287-bp *Eag*I-*Bst*EII for the D342V mutant, 794-bp *Bst*EII-*Bgl*II for the H492Y mutant, or 392-bp *Bgl*II-*Sph*I fragments for S706F and M756V mutants, respectively, for the corresponding fragments of WT/*KCNQ1* or WT/*KCNH2*.

Cell Transfection

Functional potassium channels were expressed transiently in Chinese hamster ovary (CHO) cells by transfecting the same amount of α subunit plasmids (1 μg/mL *KCNQ1* cDNA or 2 μg/mL *KCNH2* cDNA). For the analysis of I_{Ks} currents, the same amount of pIRES/CD8-*KCNE1* was coexpressed. Cells were trypsinized, diluted with Dulbecco Modified Eagle's Medium (DMEM, Nacalai Tesque, Kyoto, Japan) supplemented with 10% fetal bovine serum, 30 U/mL penicillin, and 30 μg/mL streptomycin. The DMEM used for cell culture dishes was changed to OptiMEM (Invitrogen, Carlsbad, Calif) for transfection, and, after the addition of 10 μL lipofectamine (Invitrogen) and cDNA, the cells were incubated at 37°C for 3 hours, unless otherwise described. OptiMEM was then replaced by DMEM and the cells were subjected to electrophysiological measurements 48 to 72 hours after transfection. Cells expressing the potassium channels were selected through detection of green fluorescent protein and by decoration with anti-CD8 antibody-coated beads.

Electrophysiology

Whole-cell patch-clamp recordings were made at 37°C, using an EPC-8 patch-clamp amplifier (HEKA, Lambrecht, Germany) with pipettes filled with (in mM): 70 aspartate, 70 KOH, 40 KCl, 10 KH_2PO_4, 1 $MgSO_4$, 3 Na_2-ATP, 0.1 Li_2-GTP, 5 HEPES, and 5 EGTA (pH 7.3 with 1N KOH), with a resistance of 2.0 to 4.0 mol/LΩ. The external superfusate contained (in mM): NaCl 140, KCl 5.4, $MgCl_2$ 0.5, $CaCl_2$ 1.8, NaH_2PO_4 0.33, glucose 5.5, and HEPES 5 (pH 7.4 with NaOH). Data were filtered at 2 kHz. Data acquisition was performed using PatchMaster acquisition software (HEKA). The holding potential was set at −80 mV. Current densities (pA/pF) were calculated for each cell studied, by normalizing peak tail current amplitude to cell capacitance. Current-voltage relations were fitted with the Boltzmann function:

$$I/I_{max} = 1/(1+\exp((V_{1/2}-Vm)/k))$$

where $V_{1/2}$ indicates the potential at which the activation or inactivation is half-maximal, Vm the test potential, and k the slope factor.

Drug sensitivities were examined by various concentrations for erythromycin, disopyramide, and pirmenol (gift from Pfizer Inc, Groton, Conn). Depolarizing pulses were applied every 15 seconds and peak tail currents at −60 mV after +20 mV test potential were recorded in the absence or presence of various concentrations of agent. Percent inhibition was calculated by dividing the peak amplitude in the presence of drug by control. Drug concentration-inhibition relations were fitted to the Hill equation;

$$\text{Fractional drug inhibition} = 1/(1+(IC_{50}/[\text{drug}])^n)$$

where IC_{50} is the amount of drug necessary to produce the half-maximal inhibition of I_{Kr} tail currents, and n is the Hill coefficient for the fit.

Computer Simulation

The dynamic Luo-Rudy model (Clancy and Rudy 2001 model) of a ventricular cell was used, with recent modifications and action potentials were simulated using a previously reported model.[16] The ratio of I_{Kr} and I_{Ks} conductance of M cell layer was set at 23:7. Based

on the experimental data of voltage-clamp recordings of *KCNQ1* and *KCNH2* channels heterologously expressed in CHO cells, we constructed Markov or Hodgkin-Huxley models for simulated mutant channels as compared with mutants associated with cLQTS (see supplemental data 1). To make the mutant channel models, we decreased the conductance of each channel as appropriate for the decreased current density and looked for adequate changes for mutant channels by changing each coefficient value, in turn, for gating states associated with impaired gating defects. The simulation for voltage-clamp experiments was calculated using the 4th-order Runge-Kutta method with a fixed-time step of 0.020 ms. The simulation programs (see supplemental data 1) were coded in C++ and implemented for personal computers.

Statistical Analysis

Experimental data are expressed as mean±SE and other clinical data as mean±SD, and the statistical comparisons were made using the unpaired Student *t* test. Differences in the positive mutation rate between 2 groups were analyzed by χ^2 and Fisher exact probability test. Statistical significance was considered as $P<0.05$.

Results

Molecular Genetics of dLQTS

Table 1 summarizes the clinical characteristics of 20 subjects with dLQTS (14 women and 6 men; mean age, 65±16 years). Nineteen subjects had TdP with marked QT prolongation, and 1 had syncope without documented TdP after taking 1 of the drugs listed in Table 1. The average QT_c interval before taking drugs, available for 15 subjects, was 446±29 ms. The QT_c interval was significantly prolonged to 616±91 ms after taking 1 of the culprit drugs (versus QT_c interval before taking drugs, $P<0.001$) and significantly shortened to 441±33 ms after washout of drugs (versus QT_c interval after taking drugs, $P<0.001$). However, in 3 patients (cases 8, 13, and 18 in Table 1) a prolonged QT interval of over 480 ms was maintained after washout. The average R-R interval immediately before TdP was 1.2±0.4 seconds, and the average serum potassium level after TdP was 3.9±0.6 mEq/mL. In the majority of subjects (n=14, 70%), dLQTS was induced by antiarrhythmic drugs (disopyramide, pirmenol, cibenzoline, procainamide, and aprindine in 8, 3, 1, 1, and 1 subjects, respectively; cases 1 to 14); the remaining cases were induced by antihistamines, antibiotics, psychiatric, or miscellaneous drugs (cases 15 to 20 in Table 1). None had a family history of long-QT syndrome, whereas 3 subjects (cases 4, 14, and 20) had unexplained syncope and another subject (case 17) had a family member with sudden cardiac death. During a mean follow-up period of 52±44 months after discontinuing drugs, 1 subject without any gene mutations (case 9) had recurrent ventricular fibrillation. Compared with cLQTS, the age at first cardiac event in subjects diagnosed with dLQTS was significantly older (dLQTS versus cLQTS; 65±16 versus 19±18 years, $P<0.001$). No subject in the dLQTS group had a family member with long-QT syndrome (dLQTS versus cLQTS; 0% versus 24% subjects, $P<0.01$). The QT_c interval in dLQTS subjects was significantly shorter than in cLQTS subjects (dLQTS versus cLQTS; 446±29 versus 507±71 ms, $P<0.001$); the Schwartz score was significantly lower in dLQTS than in cLQTS (dLQTS versus cLQTS; 0.9±1.4 versus 4.1±2.1, $P<0.001$).

In 8 (40%) dLQTS subjects, the genetic analysis identified 8 mutations in LQTS-related genes; 2 *KCNQ1*, 5 *KCNH2*, and 1 *SCN5A* (Table 1). These variants were not observed in the control subjects (220 chromosomes from non-cLQTS and non-dLQTS subjects), suggesting that they represented disease-related mutations. The 91 cLQTS patients also had gene mutations such as 33 *KCNQ1*, 36 *KCNH2*, 12 *SCN5A*, 2 *KCNE2*, and 8 compound mutations, and the positive mutation rate was similar between dLQTS and cLQTS subjects (8 of 20 [40%] versus 91 of 176 [52%] subjects, respectively, $P=0.32$, Figure 1A). These mutations were found in only 3 of 14 (21%) subjects with TdP induced by antiarrhythmic drugs. In contrast, 5 of 6 subjects with TdP induced by nonantiarrhythmic drugs had gene mutations (83%; versus patients with TdP induced by antiarrhythmic drugs, $P<0.05$) (Figure 1B). Seven of the 8 mutations were located in the nonpore regions (red circles in Figure 1C), except for the A614V-*KCNH2* mutation in a case of hydroxyzine-induced TdP.[17] The green circles in Figure 1C indicate the location of 8 mutations previously reported in dLQTS.[5–10]

Clinical Characteristics of Genotyped dLQTS Subjects

Detailed subject characteristics are presented in Table 1 and the supplemental data 2. Case 2 (M756V/*KCNH2*) was a 63-year-old man who was admitted with syncope after taking pirmenol (300 mg/d). Case 4 (H492Y/*KCNH2*) was a 52-year-old woman who had syncope while taking disopyramide (300 mg/d). She had previously had 1 episode of unexplained syncope. Case 14 (R243H/*KCNQ1*) was a 52-year-old woman who had repetitive syncope after taking aprindine (60 mg/d). Case 15 (S706F/*KCNH2*) was a 21-year-old woman who complained of sudden onset of palpitations and dyspnea after taking amphetamine and methamphetamine. An *SCN5A* mutation (L1825P/*SCN5A*) (case 16), has been reported previously[5]; this concerned a 70-year-old woman who had TdP and prolongation of the QT interval after taking cisapride (5 mg/d) and pirmenol (200 mg/d). Case 17 (D342V/*KCNH2*) was a 70-year-old woman who had repetitive syncope due to erythromycin intake (1200 mg/d). This subject had a 24-year-old sister who had died suddenly, but it is not unknown if her sister had suffered from LQTS. Case 18 (R231C/*KCNQ1*) was a 72-year-old woman who had presyncope while taking probucol (250 mg/d). Case 20 concerned a 34-year-old woman (A614V/*KCNH2* according to Table 1) who had syncope and QT prolongation induced by hydroxyzine (3 mg/d).[17] None of the 20 subjects in the study had structural heart disease or a family history of documented LQTS. In genotyped families, a genetic test for 5 members revealed 1 R243H/*KCNQ1* mutation carrier. This carrier had no syncope and a normal QT interval (QT_c, 400 ms). The Schwartz scores in the 8 subjects with mutations were 1.0±1.5 points (range, 0 to 4 points). Thus, among the genotyped dLQTS subjects in this current study, there was only a low or moderate possibility of LQTS being present, both before taking the drugs or after their withdrawal.

Table 1. Clinical Characteristics and Gene Mutations of Probands With Drug-Induced Arrhythmic Events

No.	Age, y	Sex	Drug Types	Culprit Drugs, Dose/d	Cardiac Events	Previous Syncope/LQTS Members	QTc, ms			Serum K, mEq/l, After TdP	R-R Interval Before TdP, s	Nucleotide Change	Mutation/Gene
							Before Taking Drugs	After Events	After Washout of Drugs				
1	68	M	Antiarrhythmic drug	Disopyramide, 300 mg	TdP	−/−	421	609	425	4.4	0.7		
2	63	M	Antiarrhythmic drug	Pirmenol, 150 mg	TdP	−/−	453	632	Normal	NA	1.1	a2266g	M756V/KCNH2
3	81	F	Antiarrhythmic drug	Disopyramide, 300 mg	TdP	−/−	447	563	456	2.8	1.3		
4	52	F	Antiarrhythmic drug	Disopyramide, 300 mg	TdP	+/−	495	585	447	3.2	1.1	c1474t	H492Y/KCNH2
5	74	M	Antiarrhythmic drug	Disopyramide, 300 mg	TdP	−/−	383	553	370	4.0	0.9		
6	86	F	Antiarrhythmic drug	Cibenzoline, 100 mg	TdP	−/−	NA	620	430	4.3	1.4		
7	56	F	Antiarrhythmic drug	Disopyramide, 300 mg	TdP	−/−	446	577	383	NA	1.2		
8	79	F	Antiarrhythmic drug	Disopyramide, 300 mg	TdP	−/−	Kent (+)	597	495	NA	NA		
9	77	M	Antiarrhythmic drug	Pirmenol, 200 mg	TdP	−/−	450	538	449	4.3	2.1		
10	69	F	Antiarrhythmic drug	Disopyramide, 150 mg	TdP	−/−	421	557	403	4.1	NA		
11	67	F	Antiarrhythmic drug	Disopyramide, 50 mg*	TdP	−/−	464	506	435	NA	1.4		
12	62	M	Antiarrhythmic drug	Pirmenol, 200 mg	TdP	−/−	430	484	424	4.1	1.0		
13	61	M	Antiarrhythmic drug	Procainamide, 200 mg*	TdP	−/−	487	705	496	4.9	NA		
14	52	F	Antiarrhythmic drug	Aprindine, 60 mg	TdP	+/−	NA	857	469	4.2	TdP on adm.	g728a	R243H/KCNQ1
15	21	F	Nonantiarrhythmic drug	3,4-Methylenedioxymethamphetamine, 10 tabs	TdP	−/−	426	600	450	3.4	TdP on adm.	c2117t	S706F/KCNH2
16	70	F	Nonantiarrhythmic drug	Cisapride, 5 mg	TdP	−/−	435	731	417	3.8	1.5	t5474c	L1825P/SCN5A
17	70	F	Nonantiarrhythmic drug	Erythromycin, 1200 mg	TdP	−/−	454	776	440 (AF)	3.9	0.9	a1025t	D342V/KCNH2
18	72	F	Nonantiarrhythmic drug	Probucol, 250 mg	TdP	−/−	480 (AF)	754	495 (AF)	3.2	1.0	c691t	R231C/KCNQ1
19	77	F	Nonantiarrhythmic drug	Haloperidol, 5 mg	TdP	−/−	NA	574	447	4.6	4.6		
20	34	F	Nonantiarrhythmic drug	Hydroxydine, 3 mg	syncope	+/−	Untested	626	449	Untested	Untested	c1841t	D614V/KCNH2
Ave±SD	65±16						446±29	616±91	441±33	3.9±0.6	1.2±0.4		

M indicates male; F, female; NA, not available; AF, atrial fibrillation; Kent (+), type A Wolf-Parkinson-White syndrome; prolonged QT, ECG shows prolonged QT interval but unspecified QT interval; normal, normal QT interval but unspecified QT interval.

*Intravenous administration.

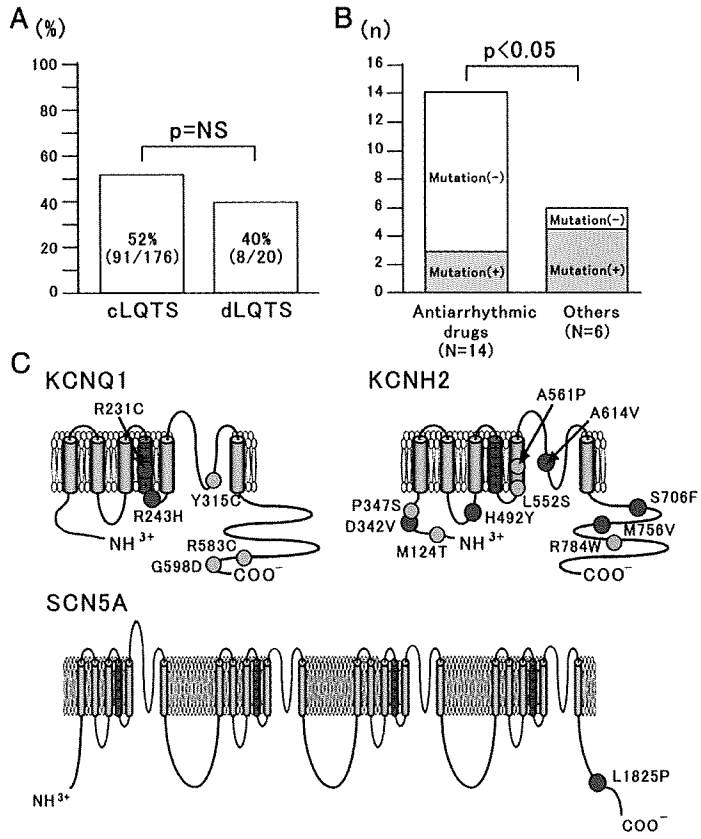

Figure 1. Molecular genetics of gene mutations in subjects with drug-induced long QT syndrome (LQTS). A, A pie graph showing the incidence of mutation carriers in our drug-induced LQTS cohort. B, Bar graph showing different mutation detection rates depending on culprit drugs. C, Schemes indicating the location associated with drug-induced LQTS. Red circles indicate the sites of mutations detected in this study; green circles indicate previously reported mutations.

Electrophysiological Characteristics of Mutations Associated With dLQTS

The biophysical effects of the respective *KCNQ1* and *KCNH2* mutations were analyzed using a heterologous expression system with the CHO cell line. The upper panel of Figure 2A shows representative current traces for WT and 2 mutant *KCNQ1* channels; the lower panel shows those recorded from cells cotransfected with WT and each mutant. On their own, both mutants displayed smaller currents compared with WT, whereas the R231C channel was a slightly open K^+ leak channel. Under heterozygous conditions, however, they displayed currents comparable to those of WT without dominant negative effects.

At the end of the depolarizing pulse to +40 mV, current densities were smaller than those of WT channels (77.0±10.6 pA/pF) in R231C/WT (39.6±11.9 pA/pF, $P<0.05$ versus WT) but not in R243H/WT (61.9±10.7 pA/pF) (Figure 2B). On the other hand, the R243H channels showed a significant positive shift of steady-state activation curve (Figure 2C). Half activation voltages ($V_{1/2}$) and k were −8.2±3.1 mV and 12.6±0.6 for WT, −12.8±3.6 mV and 13.6±1.3 for R231C/WT, 1.7±3.1 mV and 12.9±0.6 for R243H/WT, respectively ($V_{1/2}$: WT versus R243H/WT, $P<0.05$). Figure 2D shows representative families of current traces (left panel) and time constants (right panel) of deactivation in each channel. The time course of deactivating kinetics could be fitted by a single-exponential function. The R243H/WT channel had faster deactivation process over −60 mV, whereas this process in the R231C/WT channel was slower than WT under −90 mV.

Figure 3A shows representative families of current traces recorded during depolarizing pulses from CHO cells transfected with *KCNH2* cDNAs as indicated in the graph. The left column depicts current traces from cells transfected with each construct alone and the right column those recorded under heterozygous conditions except for the uppermost traces (WT 1 μg). When expressed alone, D342V was nonfunctional and 3 other mutations displayed functional channels. When coexpressed with WT, D342V showed weak dominant negative effects, whereas the other 3 channels showed nondominant negative effects. The functional outcome of the remaining mutation, A614V-*KCNH2*, [17] has recently been reported. Using an oocyte expression system, Nakajima et al[18] reported that the A614V channel showed loss of function in a dominant negative manner, and the results from the present study were almost identical (18% current density of WT).

Current densities at the end of a 2-second depolarization pulse were calculated in multiple cells and plotted as a function of test potential in Figure 3B. At the end of the depolarizing pulse to +20 mV, the densities were smaller than those of WT channels (36.2±6.8 pA/pF) in D342V/WT (18.7±4.5 pA/pF, $P<0.05$ versus WT) and S706F/WT (21.9±2.7 pA/pF, $P=0.055$ versus WT). Those in

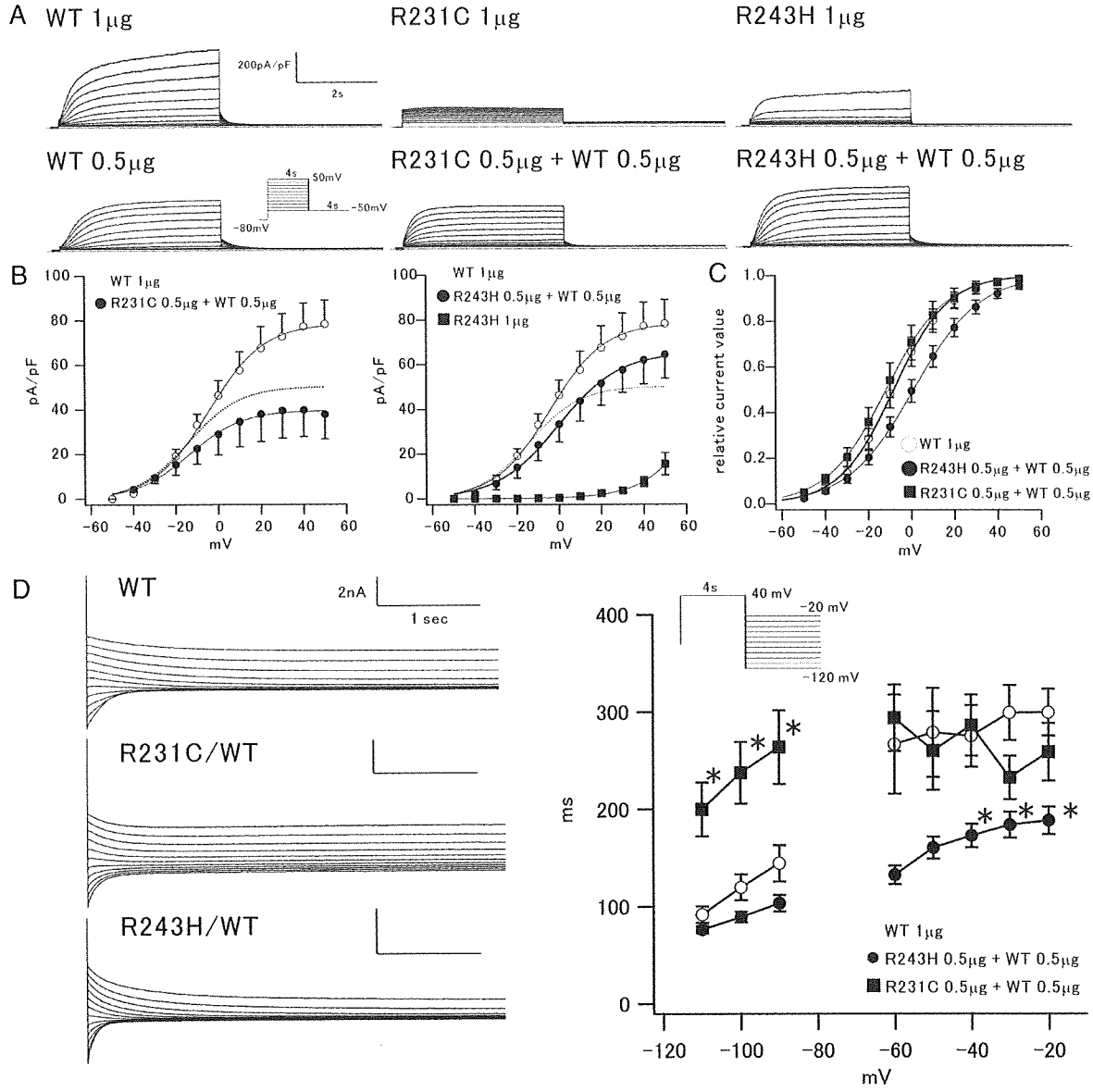

Figure 2. Mutations associated with nondominant negative effects of *KCNQ1* channels. A, Current traces reconstituted in CHO. Current amplitude was normalized by respective cell capacitance and was indicated as the current density. B, Current-voltage (I-V) relationships for amplitudes of steady-state currents at the end of 4-second depolarizing pulses. Currents were elicited by depolarizing pulses from a holding potential of −80 mV to test potential between −50 to +50 mV (with a 10-mV step increment), followed by repolarization to −50 mV to monitor tail current amplitude. The voltage-clamp protocol is shown in the inset. Open circles, WT (1 μg); filled squares, mutant (1 μg); filled circles, WT (0.5 μg) plus mutant (0.5 μg); and dotted lines, WT (0.5 μg). All data were recorded from 10 to 25 cells. C, Steady-state activation curves for WT and WT plus mutants. D, *KCNQ1* mutants modify deactivation time curse. Left column presents the time course of deactivation for each channel. Each inset illustrates scale bars of 2-nA and 1-second times. To examine the deactivation time course, a conditioning pulse to +40 mV for 4 seconds from a holding potential of −80 mV was followed by hyperpolarizing test pulses between −120 mV and −20 mV in 10-mV increments (inset in graph on right). Currents were not leak-subtracted. Deactivation time constants (tau) were measured by fitting deactivating currents during test pulses at each potential with a single exponential. *$P<0.05$ versus WT.

H492Y/WT and M756V/WT were also smaller than in the WT, but the difference did not reach statistical significance.

The mean peak amplitudes of tail currents at −60 mV on repolarization from various test potentials (2-second duration) plotted as a function of test potentials are displayed in Figure 3C. H492Y and M756V channels displayed amplitudes of peak tail currents similar to WT. For example, the peak tail current densities after a test pulse to +20 mV were 66.2±10.5 pA/pF for WT, 62.1±13.0 pA/pF for H492Y/WT, and 58.4±7.7 pA/pF for M756V/WT. On the other hand, the

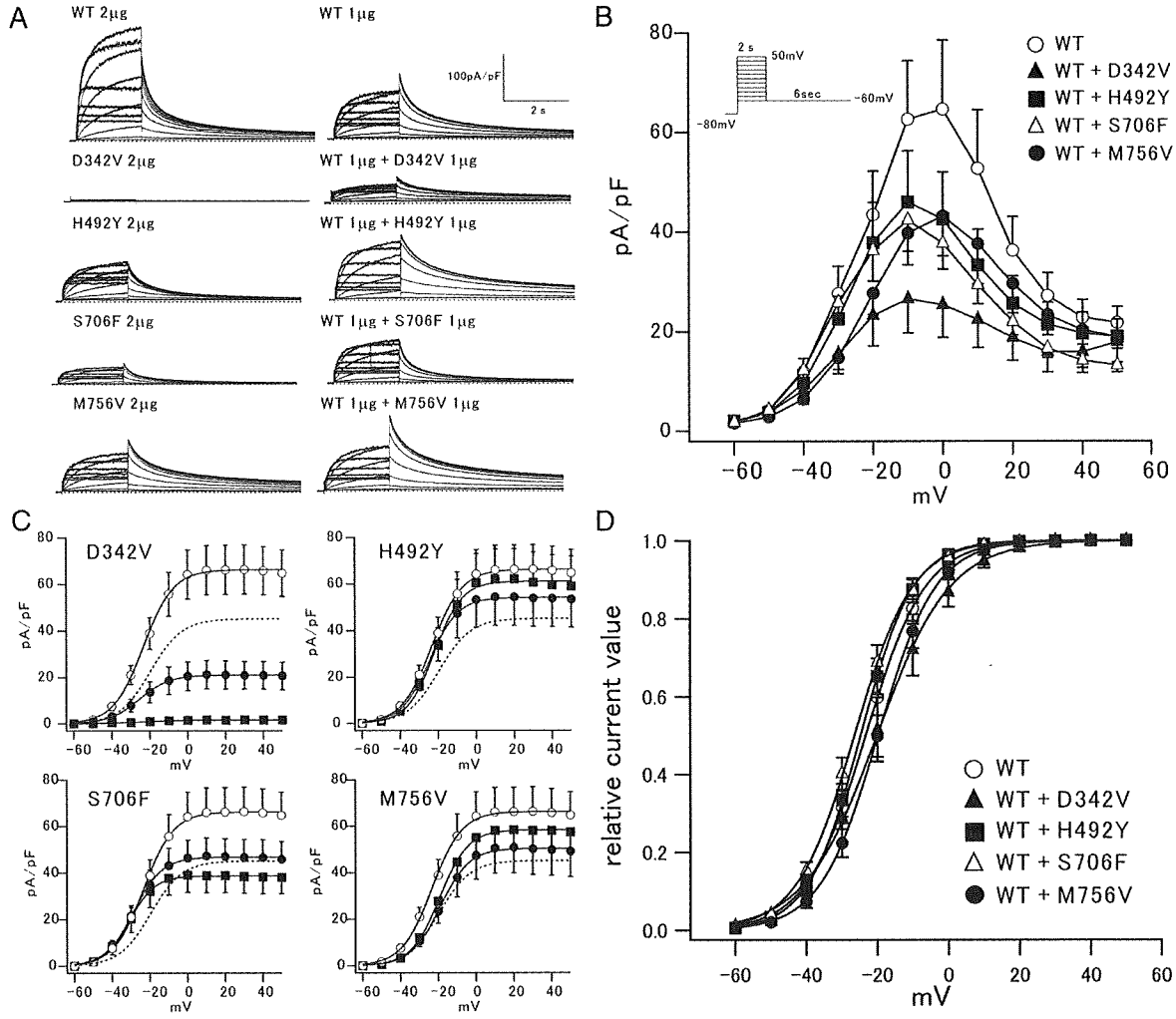

Figure 3. *KCNH2* mutations identified in drug-induced LQT subjects produced various levels of functional effects. A, Current traces of I_{Kr} reconstituted in CHO cells. Expression of the respective clones, indicated above each graph, all displayed I_{Kr}-like currents, except for D342V. Current amplitude was normalized by respective cell capacitance and was indicated as the current density. B, Current-voltage (I-V) relationships for amplitudes of steady-state currents at the end of 2-second depolarizing pulses. Currents were elicited by depolarizing pulses from a holding potential of −80 mV to test potential between −60 to +50 mV (with a 10-mV step increment), followed by repolarization to −60 mV to monitor tail current amplitude. The voltage-clamp protocol is shown in the inset. C, I-V relationships for amplitudes of peak tail currents measured at −60 mV. Open circles, WT (2 μg); filled squares, mutant (2 μg); filled circles, WT (1 μg) plus mutant (1 μg); and dotted lines, WT (1 μg). All data were recorded from 10 to 25 cells. D, Voltage dependence of activation for each channel. The data were fitted to a Boltzmann function.

current densities of D342V/WT (1.5±0.9 pA/pF, $P<0.001$ versus WT) and S706F/WT (38.9±7.3 pA/pF, $P<0.05$ versus WT) channels were significantly smaller than WT. D342V/WT channel displayed currents smaller than WT 1 μg (indicated by dotted line), whereas S706F/WT currents were similar to WT 1 μg in size. Thus, D342V channels had weakly dominant negative suppression effects on reconstituted I_{Kr}-like currents, whereas S706F had no dominant negative suppression effect. To examine the voltage dependence for activation, Boltzmann function curves were fitted to the relationship between peak tail currents and test voltages under respective conditions and are represented by solid lines in Figure 3C. Half inactivation voltages ($V_{1/2}$) were −23.2±1.6 mV for WT, −19.8±3.0 mV for D342V/WT, −24.6±1.4 mV for H492Y/WT, −26.1±1.5 mV for S706F/WT, and −19.8±1.7 mV for M756V/WT, respectively (Figure 3D). Therefore, the mutations did not affect the voltage-dependent activation of the reconstituted I_{Kr}-like channel.

Whether the mutations affected the inactivation kinetics of *KCNH2* channels was then assessed. Figure 4A shows the voltage dependence of availability of WT and mutant channels measured by a brief repolarization method (inset). With a 1-second depolarizing pulse, peak tail current amplitudes (arrow in the inset) after short preconditioning voltage pulses (5 ms) are plotted against the voltage of conditioning pulse. Mutant channels caused significant voltage shift of channel